Description

A resonant inductive position sensor for measuring over a full 360° of rotation. Works with CambridgeIC's Central Tracking Unit (CTU) chips to provide high-quality position data to a host device.

The sensor has two sets of sensor coils: one for taking fine incremental measurements at high accuracy and resolution and another for coarse, absolute measurements. The sensor is Type 6, Subtype 3 (Type "6.3").

The sensor is connected to a CambridgeIC CTU chip, which combines the information from both sets of coils to deliver an absolute, high accuracy and high resolution output to a host system.

Features

Sensor

- Full absolute sensing over 360°
- 6-layer PCB process
- 15mm hole, e.g. for through shaft
- 34.2mm diameter copper coil pattern
- Target can be sensed from front or rear of PCB

Target

- Simple design using SMD PCB assembly
- Balanced for immunity to misalignment
- No hole required for the rotating shaft: can be mounted from the side
- Buy from CambridgeIC or build from components

Performance

Table 1 Performance

	Condition		
	Best	**Realistic installation tolerances**	**Big Gap**
Gap Sensor to Target Coils	0.5mm	1.0±0.5mm	3mm
Radial Misalignment	0mm	0.5mm	0.5mm
Angular Misalignment	0°	±0.3°	±0.3°
	Result		
Max Linearity Error	±0.15°	±0.22°	±0.3°
Noise Free Resolution	14 bits	13.3 bits	12.5 bits

Applications

- Azimuth and tilt sensing for surveillance cameras
- Motion control
- Actuator position feedback
- Valve position sensing
- Absolute Optical Encoder replacement
- Motor control, with CAM502 CTU chip

Product identification	
Part no.	**Description**
013-0024	Assembled sensor
013-6001	6-way sensor connecting cable
010-0057	Sensor Blueprint
013-1019	35mm C Target, 182.5kHz
013-1704	20mm Transponder Coil

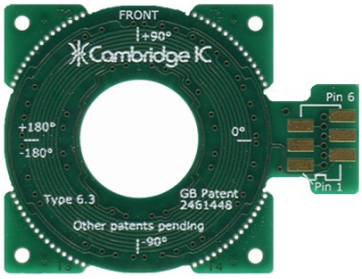


Figure 1 sensor 013-0024 (without connector)

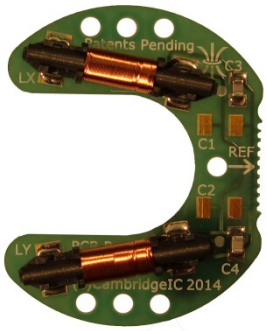


Figure 2 Assembled Target 013-1019, FRONT

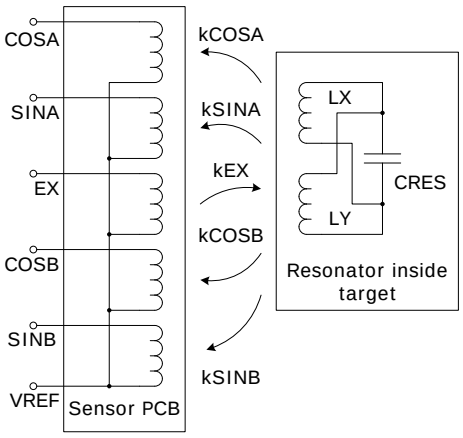


Figure 3 equivalent circuit

© Cambridge Integrated Circuits Ltd 2012-2016

1 Assembled Sensor

Figure 4 is a dimensioned drawing of the assembled sensor PCB part number 013-0024.

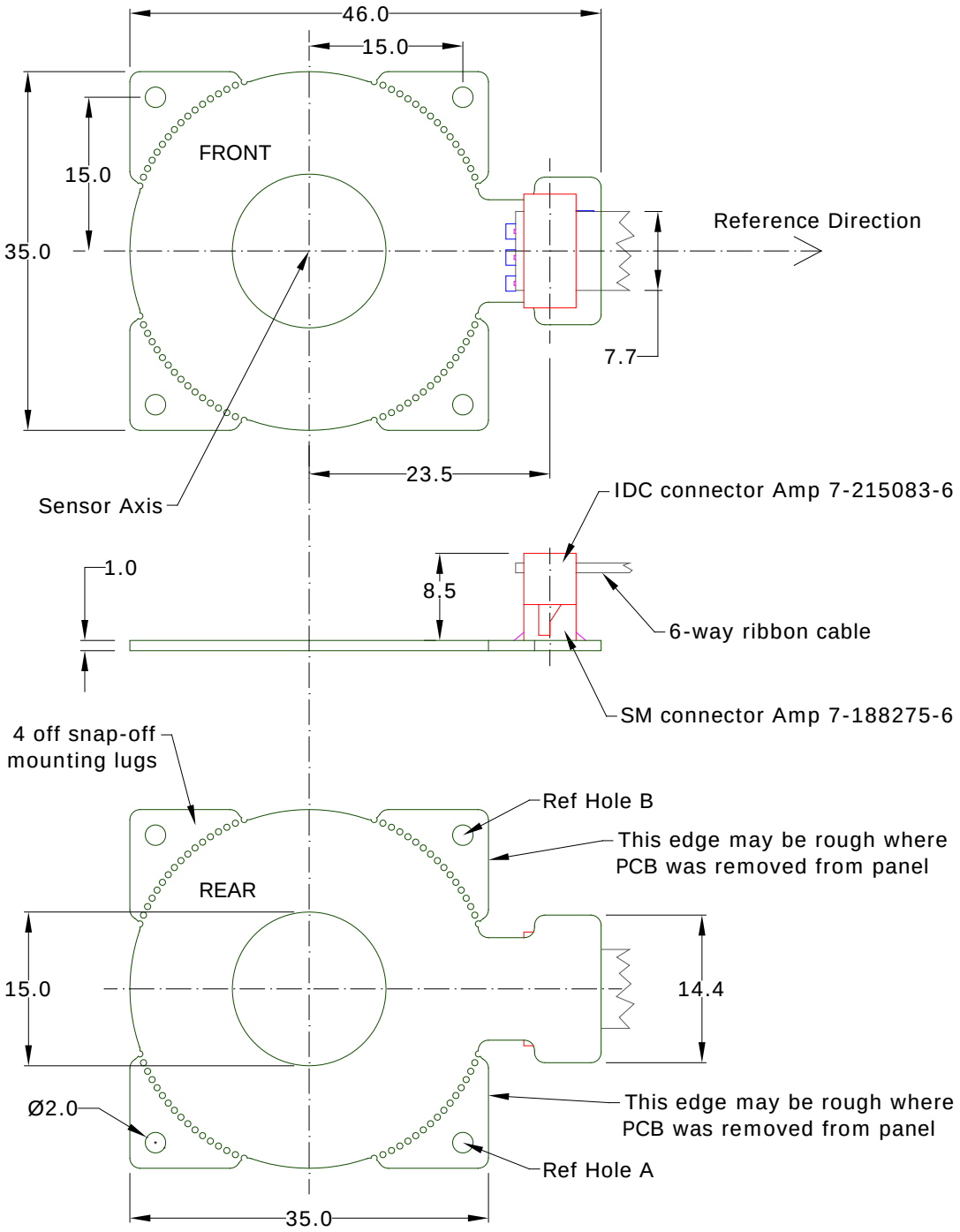


Figure 4 Assembled Sensor 013-0024 shown mated with connector 013-6001

The nominal location of the Sensor Axis is defined as 15.0mm to the left of mid way between Ref Hole A and Ref Hole B. The Reference Direction is perpendicular to the line joining the centres of these two holes.

The actual location of the Sensor Axis may be up to 0.2mm from the Nominal Sensor Axis due to hole location tolerances relative to the copper sensing pattern inherent in the PCB production process. When performance is quoted at a Radial Misalignment of 0.5mm, for example in Table 1, this 0.5mm is *in addition to* the 0.2mm misalignment

© Cambridge Integrated Circuits Ltd 2012-2016

between actual and Nominal Sensor Axis. In this case an allowance of 0.7mm has been made for the radial misalignment between the centroid of the copper pattern and the Target Axis.

The assembled sensor part number 013-0024 includes a connector mounted on the rear, located as shown in Figure 4. Table 2 shows signal names and their pin allocations.

Table 2 Sensor Assembly electrical connections

Pin no	Signal name
1	EX
2	CB
3	SB
4	CA
5	REF
6	SA

Any of the four mounting lugs may be snapped off if required, for example to save space. Support the centre of the sensor on a flat surface with the lug overhanging an edge, grip the lug with pliers and bend the lug downwards over the edge. When all four of the lugs are removed the sensor dimensions are as shown in Figure 5.

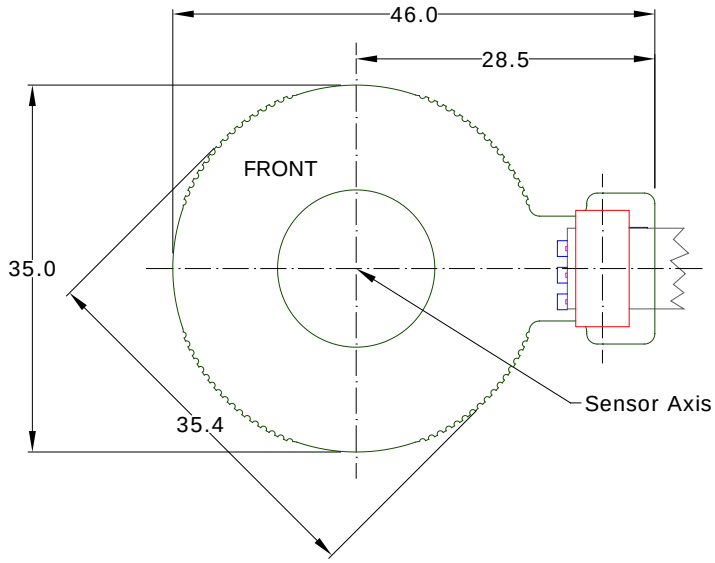


Figure 5 Assembled sensor with mounting lugs snapped off

© Cambridge Integrated Circuits Ltd 2012-2016

2 Principle of Operation

The 35mm Type 6.3 Rotary Sensor measures the full, absolute angle of a target without contact, with high resolution and accuracy and with minimal influence of misalignment. This section illustrates how these features are achieved.

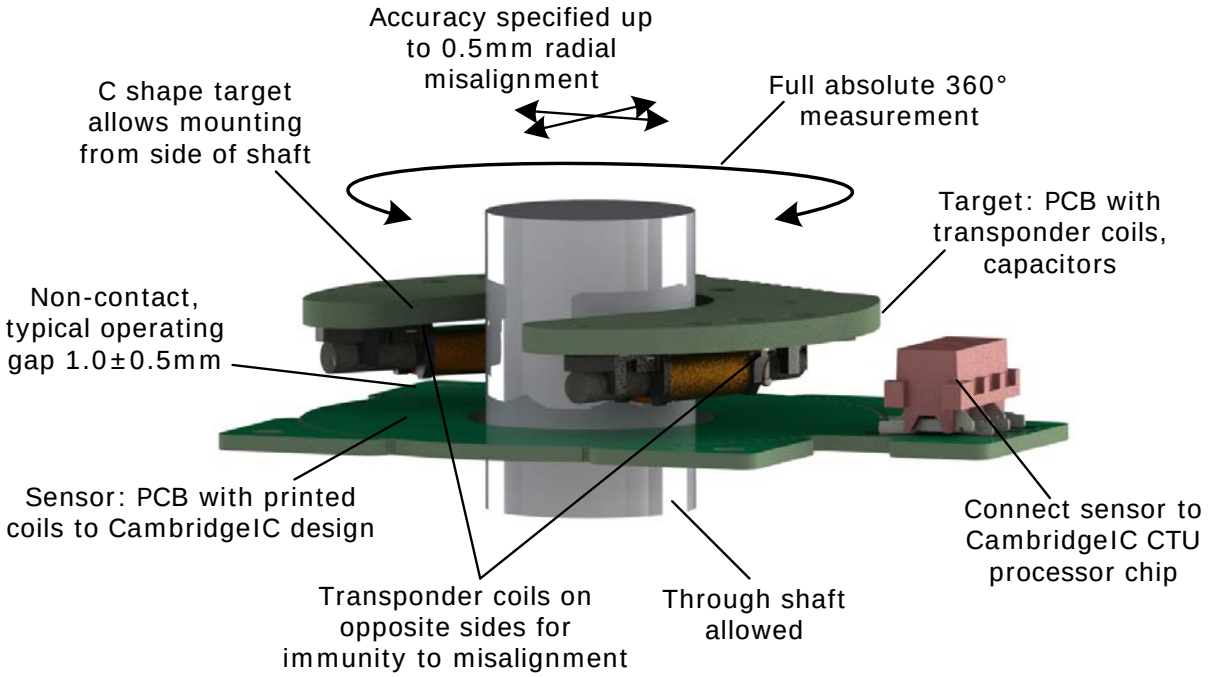


Figure 6 35mm Type 6.3 Sensor and Target function illustration

2.1 Overview

The sensor PCB comprises 5 printed coils: COSA, SINA, COSB, SINB and EX. Its equivalent circuit is illustrated in Figure 3. All 5 coils couple to a resonant circuit positioned above the sensor. The resonant circuit is the functional element inside the target, and rotates relative to the sensor.

The EX coil is for exciting this resonator. The magnetic coupling between excitation coil and resonator is uniform with rotation angle, so that the excitation coil powers the resonator whatever the rotation angle.

The other 4 coils are sensor coils, and are patterned so that their coupling factors to the resonator vary sinusoidally, as shown in section 2.3. The CTU circuit connected to the sensor detects the coupling factors and uses them to determine position.

The resonator comprises two 20mm Transponder Coils placed on opposite sides of the Target Reference Direction, shown in Figure 14. This balanced arrangement is for immunity to misalignment, see section 2.4.

© Cambridge Integrated Circuits Ltd 2012-2016

2.2 Electronic Interrogation

The sensor is connected to a CambridgeIC CTU chip (e.g. the CAM204) and its associated circuitry. To take a position measurement the CTU chip first generates a few cycles of AC current in the EX coil matching the resonant frequency of the resonator. This current forces the resonator to resonate. When the excitation current is removed the resonator continues to resonate, with its “envelope” decaying exponentially as shown in Figure 7. This decaying signal generates EMFs in the 4 sensor coils. The CTU chip detects the relative amplitude of the decaying resonator signal in each coil. It uses the amplitude information to determine position, as described below in section 2.3.

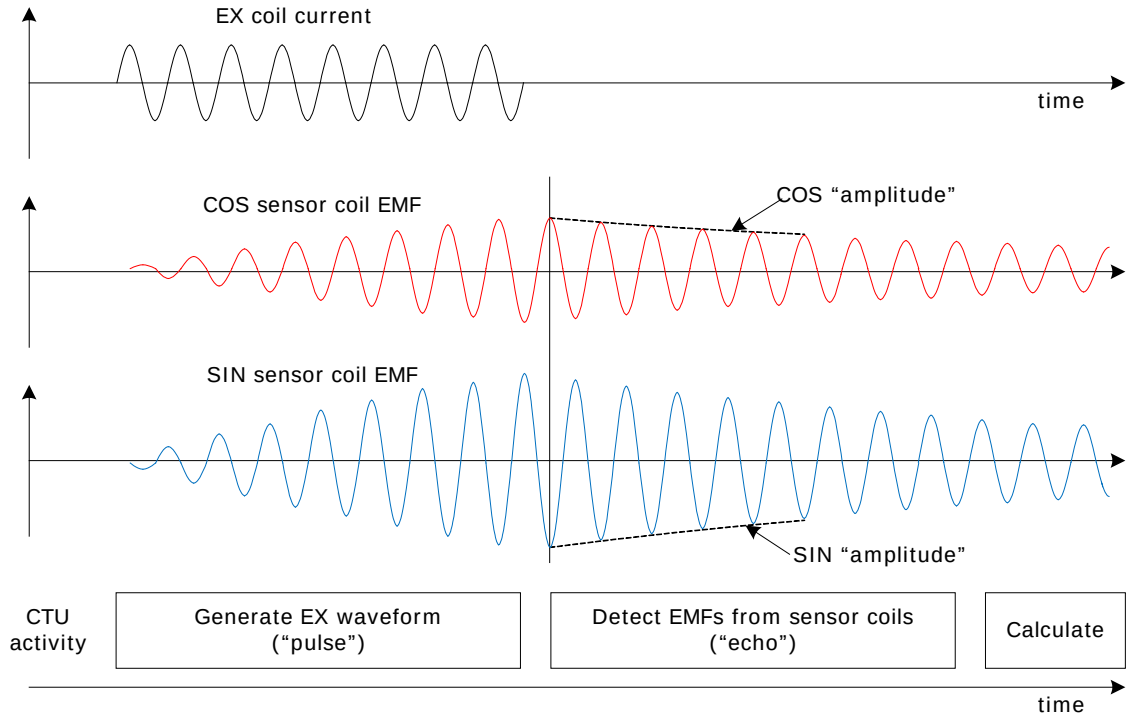


Figure 7 Electronic interrogation process

© Cambridge Integrated Circuits Ltd 2012-2016

2.3 Sensor Coils and Position Calculation

Section 0 described how the CambridgeIC CTU chip detects the relative amplitude of the signals induced by the resonator in the sensor's 4 sensor coils. These measured amplitudes are proportional to the coupling factors between the resonator and each of the 4 sensor coils, kCOSA, kSINA, kCOSB, kSINB. This subsection describes how these coupling factors change with measured angle, and the calculation the CTU chip performs to determine this angle.

Figure 8 is a simplified illustration of the sensor board's excitation coil (EX). The CTU circuit energises the target by driving a current in the EX coil. This generates a magnetic field which is positive ("+") inside the inner loops, and negative ("-") outside. The target's transponder coils lie across the excitation coil, angled so that excitation field flows through them from the inside to the outside of the sensor. The ends of the transponder coils are thus magnetised by the excitation field, with the inner portions of the transponder coils having positive polarity and the outside having negative polarity. The coupling between the excitation coil and the transponder coils in the target is uniform with Actual Angle, so that the target is uniformly powered irrespective of angle.

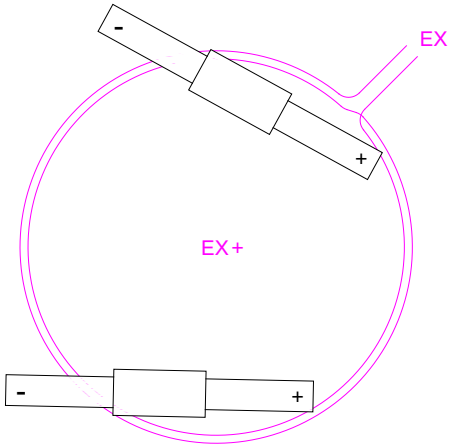


Figure 8 EX Coil, simplified

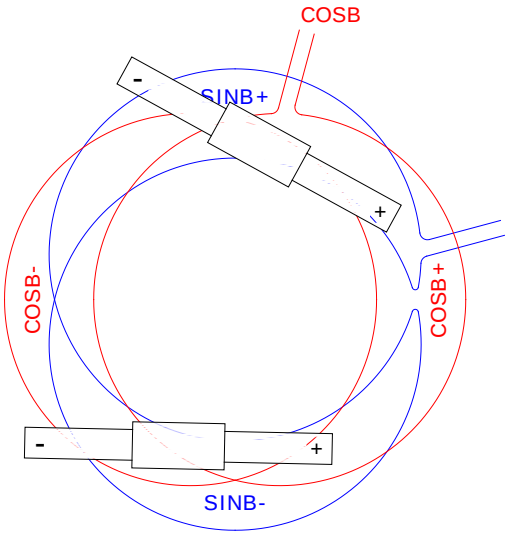


Figure 9 COSB and SINB coils, simplified

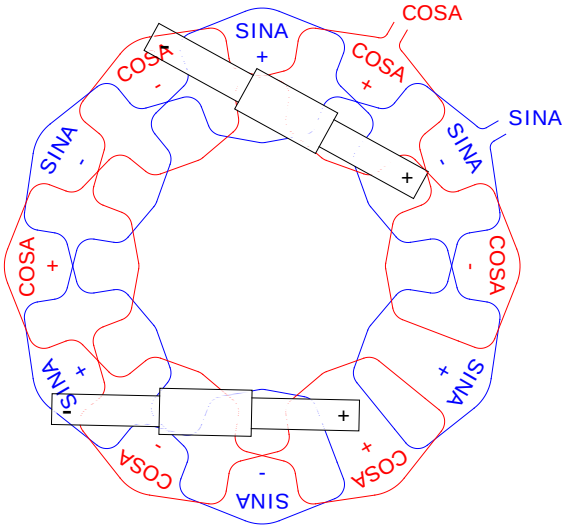


Figure 10 COSA and SINA coils, simplified

A simplified version of the COSB and SINB coils are shown in Figure 9 together with the transponder coils of the target. The COSB coil is patterned to generate an output whose amplitude varies sinusoidally with Actual Angle, and having one sinusoidal repeat per circle (*SinLengthB*=360°). The SINB coil is similar, only mechanically rotated by 90° to generate an output in the SINB coil whose amplitude varies in phase quadrature with the Actual Angle.

© Cambridge Integrated Circuits Ltd 2012-2016

The net coupling factors kCOSB and kSINB vary in a sinusoidal fashion with Actual Angle as shown in Figure 11. The CTU chip measures kCOSB and kSINB and determines *coarse position* from a 4-quadrant inverse tangent function. Coarse position is an approximate measure of angle. It is absolute across 360°.

The fine sensor coils, COSA and SINA, are shown simplified in Figure 10. They are superimposed on the EX, COSB and SINB coils. They are patterned for sinusoidal variation in coupling with angle, but this time with 3 sinusoidal repeats per 360° (SinLengthA = 120°). This number, 3 sinusoidal repeats per circle, is the sensor's Subtype.

At the Actual Angle illustrated in Figure 10, the signal amplitude measured in the SINA coil is negative, since the + ends of the transponder coils are close to the SINA- lobes, and the – ends of the transponder coils are close to the SINA+ lobes. The signal amplitude measured in the COSA coil has a similar magnitude but is positive.

The net coupling factors kCOSA and kSINA vary with Actual Angle as shown in Figure 11. The CTU chip measures kCOSA and kSINA and determines *fine position* from a 4-quadrant inverse tangent function. Fine Position is a precise measure of Actual Angle, but it is incremental across 360°, repeating 3 times (SinLengthA = 120°). The 4-quadrant inverse tangent calculation is ratiometric so that the system is immune to changes in amplitude, for example due to changes in gap and temperature.

The CTU chip combines fine and coarse position indications, so that its final output to the host has the accuracy and resolution of the "fine" reading and full absolute information from the "coarse".

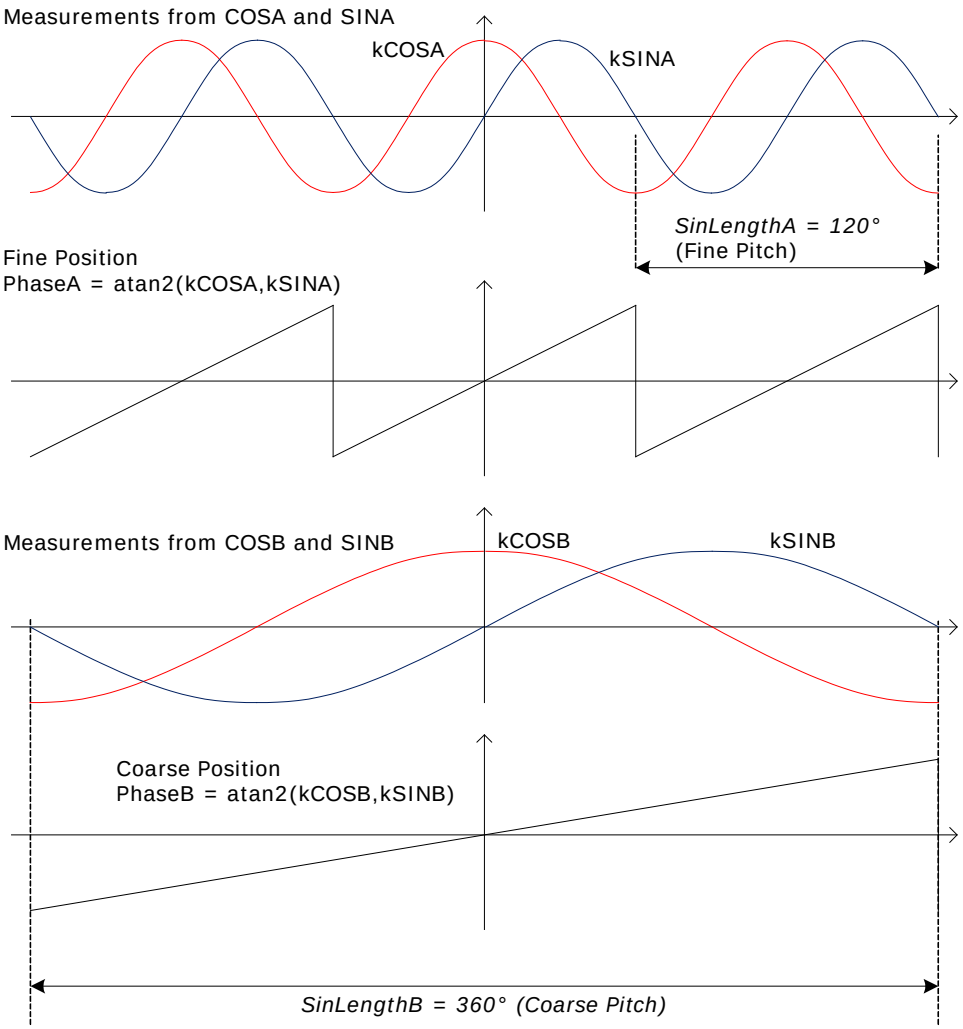


Figure 11 sensor coil coupling factors and position calculation for Type 6.3 sensor

© Cambridge Integrated Circuits Ltd 2012-2016

2.4 Immunity to Misalignment

The target described in section 3 comprises two transponder coils which are on opposite sides of the Sensor Axis. This makes the system largely immune to Radial Misalignment between the Target Origin and Sensor Axis.

The reason for this immunity is illustrated in Figure 12. Two target locations are shown, having the same Actual Angle but one without misalignment (transponder coils shown in white) and one with Radial Misalignment (transponder coils in grey). The effective angle of transponder coil X shifts by an amount *Angle X Shift*, and of transponder coil Y by *Angle Y Shift*. The system does not independently measure the effective angle of each transponder coil; by design it measures the average of the two. And since Angle X Shift is approximately equal and opposite to Angle Y shift, the two cancel leaving the system reporting approximately the same angle, unaffected by the Radial Misalignment.

The effect of Radial Misalignment is greater in the presence of angular misalignment between the target and Sensor Axes, in the AXr direction (AXr is defined in Figure 16). In this case transponder coils X and Y are no longer the same distance to the sensor, so that their relative contributions to the system's angle measurement is no longer equal and the cancellation of Angle X Shift with Angle Y shift is no longer so precise. This is why the sensor's performance is determined in the presence of both radial and angular misalignment to yield practical, worst-case figures (Table 1, section 5).

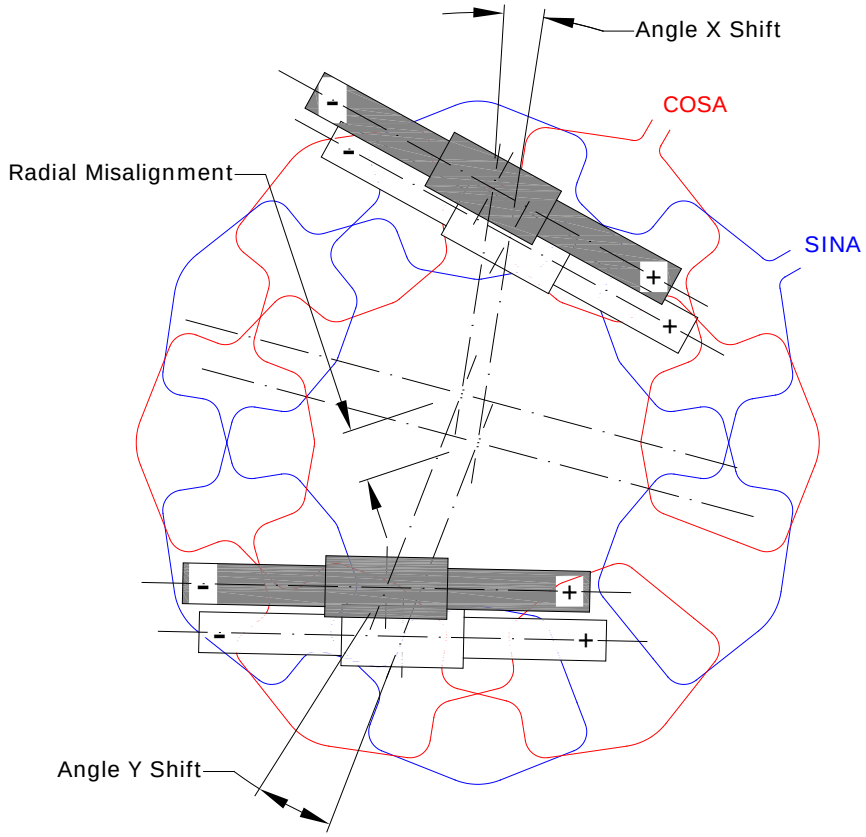


Figure 12 immunity to misalignment

Radial Misalignment causes a much larger change in coarse position, since the coarse sensor coils detect a different location on each transponder coil which is not balanced in the same way. However this has no effect on the reported position, because the coarse coils are only used to detect position to within one fine period. Absolute position reported by the CTU chip comes only from the fine sensor coils, and there is minimal change in reported position for small lateral misalignments. However very large misalignments can cause errors in reported position readings (section 5.4), and the sensor and target should be mounted to avoid these extremes.

© Cambridge Integrated Circuits Ltd 2012-2016

3 Target Design

3.1 Electrical

The 35mm Type 6.3 Rotary Sensor is designed to work with an inductively coupled resonant target comprising 2 off 20mm Transponder Coils LX and LY connected to capacitance CRES as illustrated in Figure 13.

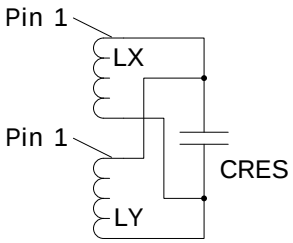


Figure 13 Schematic for target

Resonant frequency, Fres, should usually match the Nominal Operating Frequency of the CTU chip processing the sensor. Fres given by Equation 1.

$$Fres = \frac{1}{2\pi\sqrt{CRES \times LRES}}$$

Equation 1

CRES is the total resonating capacitance (the sum of the parallel connected resonating capacitors if more than one capacitor is used).

LRES is the combined inductance of the parallel connected transponder coils. These each have nominal inductance LX=LY in free space. When connected together according to Figure 13 and located as in Figure 14 the combined inductance is given by…

$$Lres = \frac{LX}{2} \times 0.982$$

Equation 2

LX is divided by 2 because the inductors LX and LY are connected in parallel. The factor 0.982 accounts for the mutual coupling between inductors LX and LY, which tends to reduce the value of their combined inductance.

When the target is integrated with metal parts, LRES should be the inductance in the presence of metal. CRES may comprise two or more capacitors connected in parallel. CRES should be formed with a stable, high Q-factor dielectric capacitor(s) such as NPO or COG, and have an operating voltage of at least 200V. The combined capacitance and inductance tolerance, including temperature effects, must yield values of Fres within Tuning Range of the CTU chip. Please refer to the CambridgeIC white paper “Resonant Frequency Centering” for more details.

© Cambridge Integrated Circuits Ltd 2012-2016

3.2 Transponder Coil Locations

To function correctly with the 35mm Type 6.3 Rotary Sensor and deliver the specified performance, locations and angles of the Transponder Coils must be as illustrated in Figure 14, and they must be mounted flush with the target PCB.

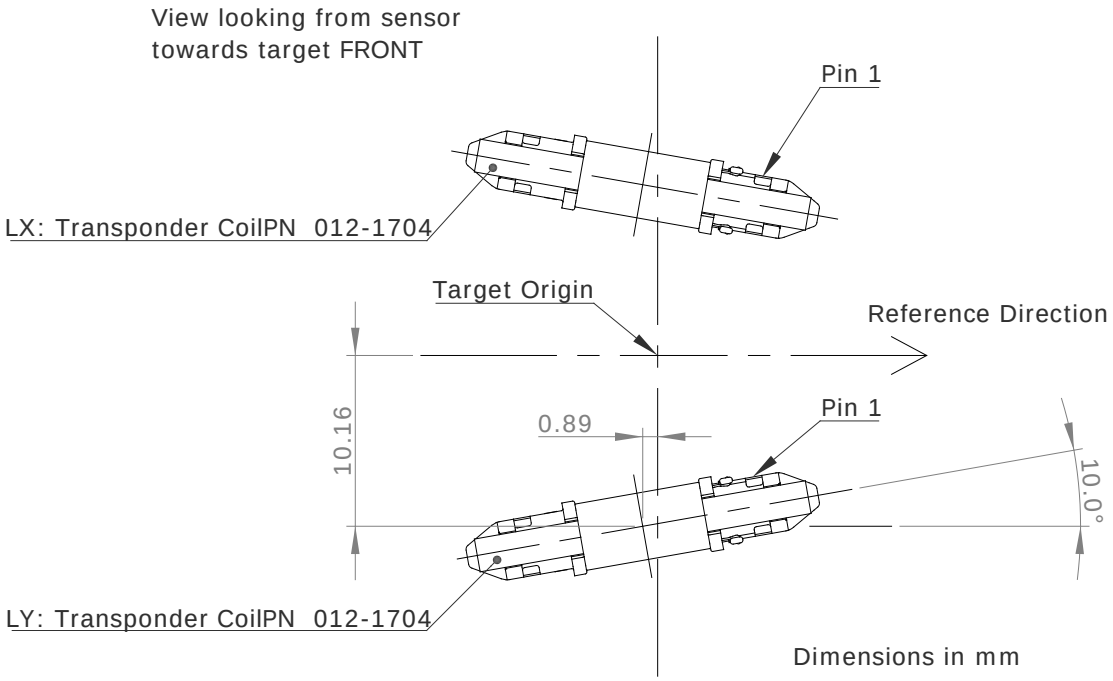


Figure 14 Transponder Coil Locations

The electrical winding direction of the two transponder coils is shown in Figure 13, with pin 1 of each part connected together. The mechanical orientation of the transponder coils is illustrated in Figure 14. It is essential that the parts are connected and oriented this way round for the target to work.

20mm Transponder Coils are surface mounted components (SMD), to enable targets to be manufactured by customers using a conventional PCB process. Please refer to their datasheet for more details. They are available to buy from CambridgeIC.

© Cambridge Integrated Circuits Ltd 2012-2016

3.3 Assembled Target

Assembled targets are also available from CambridgeIC, as illustrated in Figure 2. The mechanical design of assembled targets is shown in Figure 15. The Target Origin is defined as mid-way between the centre of Ref Hole A and Ref Hole B. The Reference Direction is perpendicular to a line joining their centres. There are a total of 7 holes that may be used for mounting and/or alignment.

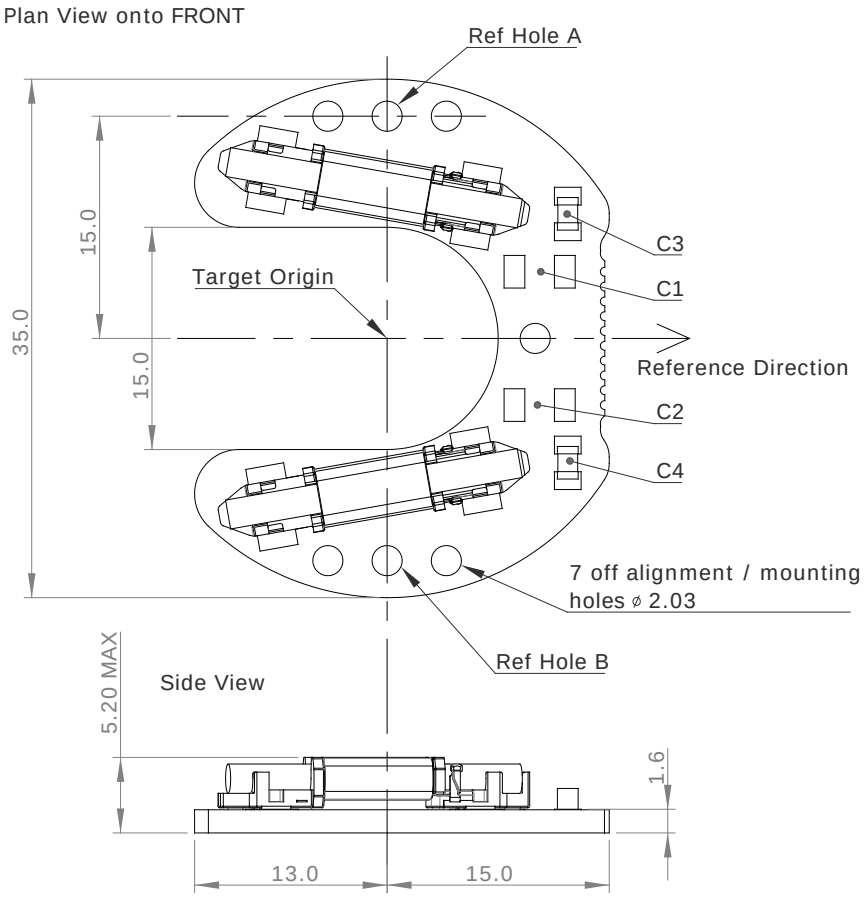


Figure 15 Assembled Target 013-1019 mechanical design

Assembled targets may be fitted with different values of capacitors, for different free space resonant frequency and hence compatibility with different metal environments. Their corresponding part numbers are shown in Table 3.

Table 3 Transponder Coil Based Assembled Targets

Part Number	**013-1019**
Fres, free space	182.5kHz (1)
Fres tolerance, 20°C	±2.5%
Fres tolerance, -40°C to +85°C	±4.5%
C1	Not fitted
C2	Not fitted
C3	1.5nF COG/NPO 250V
C4	150pF COG/NPO 250V

Note (1) For operation with the CAM204 across -40°C to +85°C in metal environments that increase resonator frequency by up to 5%.

Please contact CambridgeIC to enquire about assembled targets with different nominal values of Fres.

© Cambridge Integrated Circuits Ltd 2012-2016

4 Definitions

4.1 Coordinate System

The system measures the angle of a target relative to a sensor. The Target Reference Direction is defined in Figure 14. For assembled sensors, the Sensor Reference Direction is defined relative to REF Hole A and Ref Hole B shown in Figure 4. The Actual Angle is the angle between the two. Strictly, since the target may be slightly tilted relative to the sensor, Actual Angle is the angle between the projection of the Target Reference Direction onto the sensor's XY plane and the Sensor Reference Angle. This is denoted Actual Angle below.

The sensor's X Axis coincides with the Sensor Reference Direction, and its Y-Axis is orthogonal and in the plane of the sensor, as shown in Figure 16. The Z-Axis is orthogonal to X and Y Axes.

The target's X-Axis is denoted Xr and coincides with the Target Reference Direction. The target's Y-Axis, Yr, is orthogonal to Xr and also in the plane of the Target PCB. Tilt of the target relative to the sensor is defined about Xr and Yr. References to Angular Misalignment below are either AXr or AYr, whichever has the worst effect on linearity.

Radial Misalignment is the distance between the Target Origin and Nominal Sensor Axis.

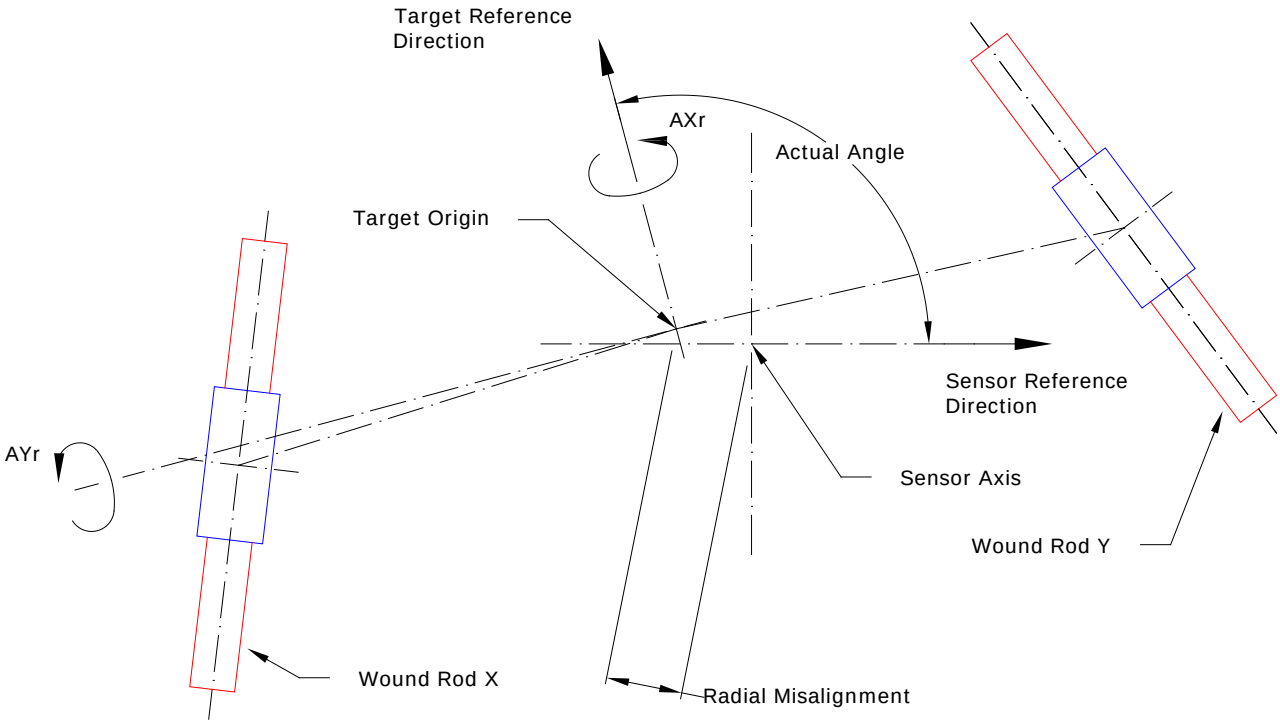


Figure 16 Coordinate System

© Cambridge Integrated Circuits Ltd 2012-2016

4.2 Gap Definition

Figure 17 shows how Gap is defined. It is the distance between sensor PCB and target PCB FRONT surfaces minus 3.5mm. That way, Gap equals the physical gap when the transponder coils are their nominal height of 3.5mm.

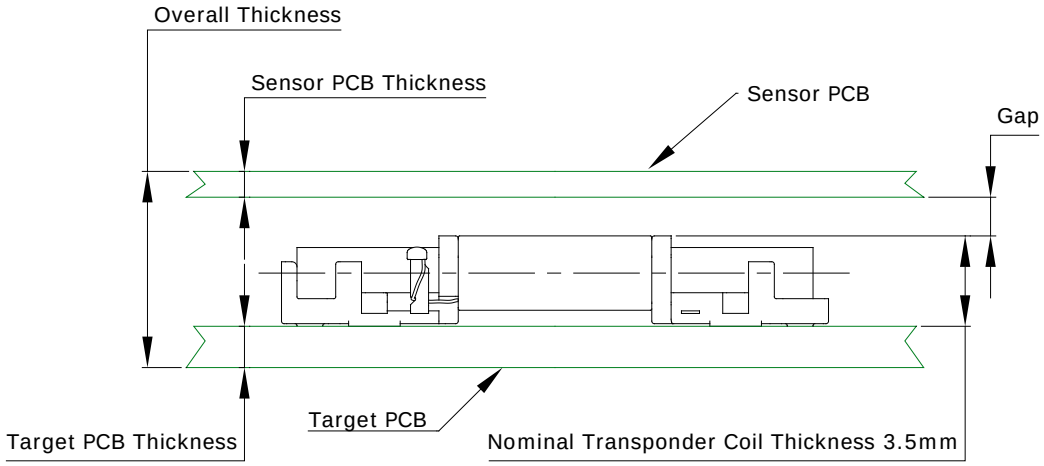


Figure 17 Definition of Gap

4.3 Transfer Function and Performance Metrics

The sensor is connected to a CTU chip which reports position as a 32-bit signed integer, here denoted *CtuReportedPositionI32*. The sensor's *Sin Length* parameter is 120°. The reported position may be converted to degrees using:

$$Reported\ Angle\ in\ Degrees = \frac{CtuReportedPositionI32}{65536} \times 120°$$

Equation 3

This figure is nominally equal to the Actual Angle defined in section 4.1. The figures differ due to random noise, Linearity Error and Offset Error:

$$Reported\ Angle - ActualAngle = RandomNoise + LinearityError + OffsetError$$

Equation 4

4.4 Random Noise and Resolution

Random noise is inherent in any analog measurement. The random noise present in the CTU's reported measurements can be considered Gaussian (*well behaved noise*). There are two general measures of Random Noise, Peak to Peak Noise and Standard Deviation. Defining Peak to Peak Noise such that it encompasses 99.9% of samples (100% is physically impossible due to the statistical nature of noise) yields the following relationship:

$$Peak\ to\ Peak\ Noise = 6.6 \times Standard\ Deviation$$

Equation 5

Another common measure of noise used in encoders is Noise Free Resolution, which is related to Peak to Peak Noise as follows:

$$Noise\ Free\ Resolution = \log_2 \frac{360°}{Peak\ to\ Peak\ Noise\ in\ °}$$

Equation 6

Noise Free Resolution can be improved by averaging raw samples from a CTU, or applying some other digital filter to the samples. Averaging 2^N samples increases Noise Free Resolution by N/2 bits. So averaging 4 samples (N=2) improves Noise Free Resolution by 1 bit, and averaging 16 (N=4) samples improves Noise Free Resolution by 2 bits. Measurements of Linearity Error and Offset Error are separated from Random Noise by averaging in this way.

© Cambridge Integrated Circuits Ltd 2012-2016

4.5 Linearity Error and Offset Error

Linearity Error is the deviation of the transfer function from a straight line. In this case the slope of the straight line is fixed at 360° per 360° because of the continuous rotary nature of the sensor. So Linearity Error simply measures deviations relative to an Offset Error.

There are two main contributions to Offset Error: one from the sensor and one from the target.

The target's contribution to Offset Error is mainly due to the location and symmetry of its transponder coils relative to the Target Reference Direction.

The sensor's contribution to Offset Error is mainly due to the PCB manufacturing process, in particular angular misregistration of layers 2, 3, 4 and 5 relative to the holes defining the Sensor Reference Angle.

4.6 Sensitivity to Radial Misalignment

Sensitivity to Radial Misalignment is measured by comparing Reported Position values with and without Radial Misalignment, and expressing the result in "angle per distance" units using…

$$Measured\ Sensitivity\ to\ Radial\ Misalignment = \frac{Reported\ Position(with\ Radial\ Misalignment) - Reported\ Position\ (no\ Radial\ Misalignment)}{Radial\ Misalignment}$$

Equation 7

This depends on Actual Angle, Angular Misalignment, Gap and so on, so typically a worst case value is presented.

When applied to an optical or magnetic encoder without the benefit of a balanced design, the worst case sensitivity is given by…

$$Imbalanced\ Sensitivity\ to\ Radial\ Misalignment = \frac{180°}{\pi} \times \frac{1}{Code\ Radius}$$

Equation 8

…where Code radius is the working radius of the code disc's optical or magnetic patterning. When comparing performance between the 35mm Type 6.3 Rotary Sensor and an optical or magnetic encoder of similar size, the Code Radius is taken to be the average of the outer and inner radii of the sensor…

$$Imbalanced\ Reference\ Sensitivity\ to\ Radial\ Misalignment = \frac{180°}{\pi} \times \frac{2}{(Outer\ Radius + Inner\ Radius\ )}$$

Equation 9

The Radial Misalignment Rejection Ratio can then be defined, comparing measured performance to expected performance for an alternative encoder system that does not benefit from balance…

$$Radial\ Misalignment\ Rejection\ Ratio = \frac{Imbalanced\ Reference\ Sensitivity\ to\ Radial\ Misalignment}{Measured\ Sensitivity\ to\ Radial\ Misalignment}$$

Equation 10

© Cambridge Integrated Circuits Ltd 2012-2016

5 Performance

Figures below are representative of assembled sensors available from CambridgeIC (as described in section 1) and of sensors built to the same specification. Measurements are taken with a typical target (built according to section 3) and CAM204 CTU Circuitry (see CTU datasheet, grade A components), at room temperature and in free space unless otherwise stated. Sensors are mounted flush against a flat surface for test purposes.

Measurements are presented as a function of Gap, which is defined in section 4.2.

5.1 Linearity Error

Linearity Error is defined in section 4.5. It is minimised when there is no Radial or Angular Misalignment. Figure 18 shows how Linearity Error changes with Gap and when misalignments are introduced. The quoted misalignment is *in addition* to ±0.2mm of misalignment between copper and REF Holes.

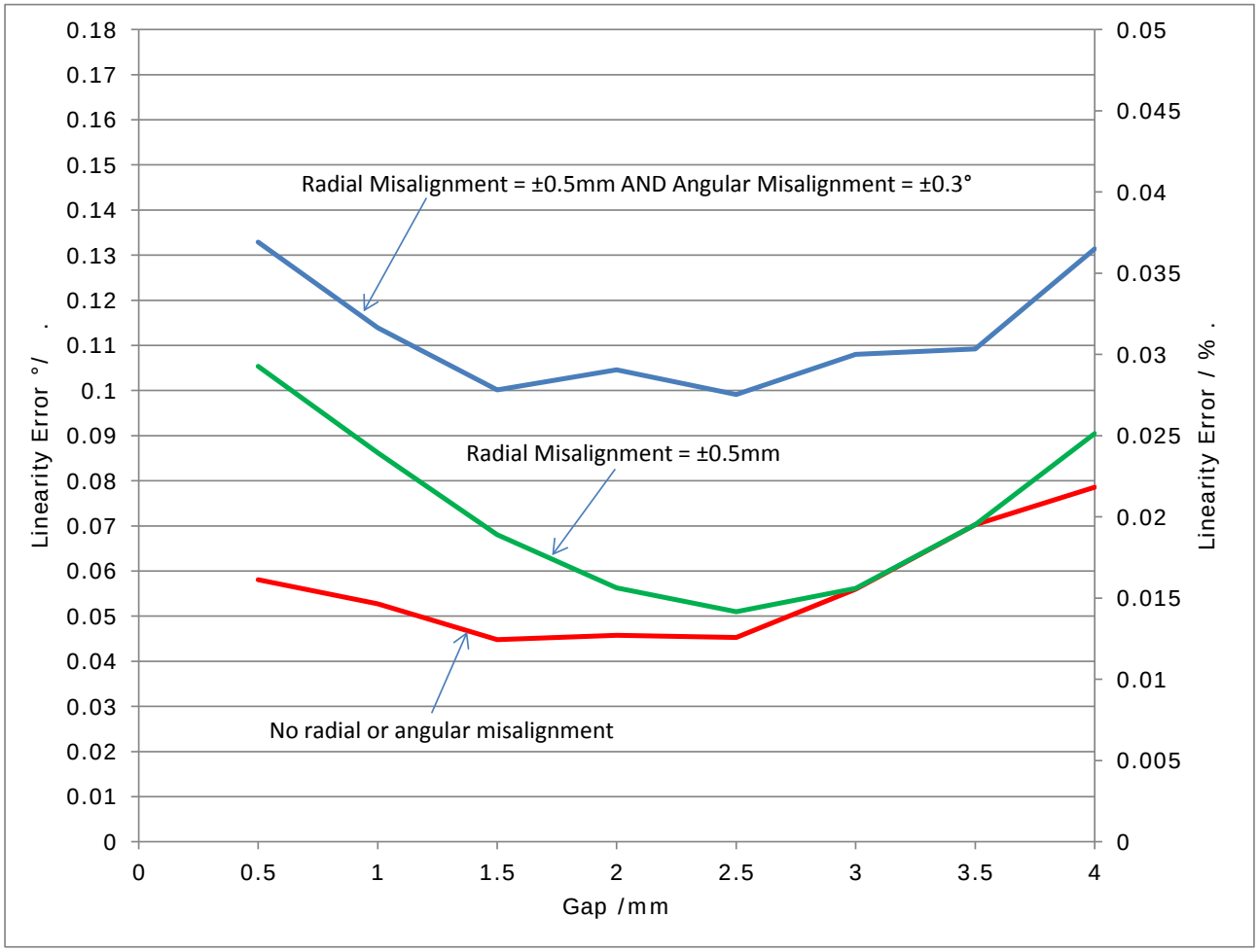


Figure 18 Linearity Error as a function of Gap and misalignment

© Cambridge Integrated Circuits Ltd 2012-2016

5.2 Amplitude

In addition to reporting position, the CTU chip also reports Amplitude. Amplitude is a useful measure of system health, and reduces with gap as shown in Figure 19.

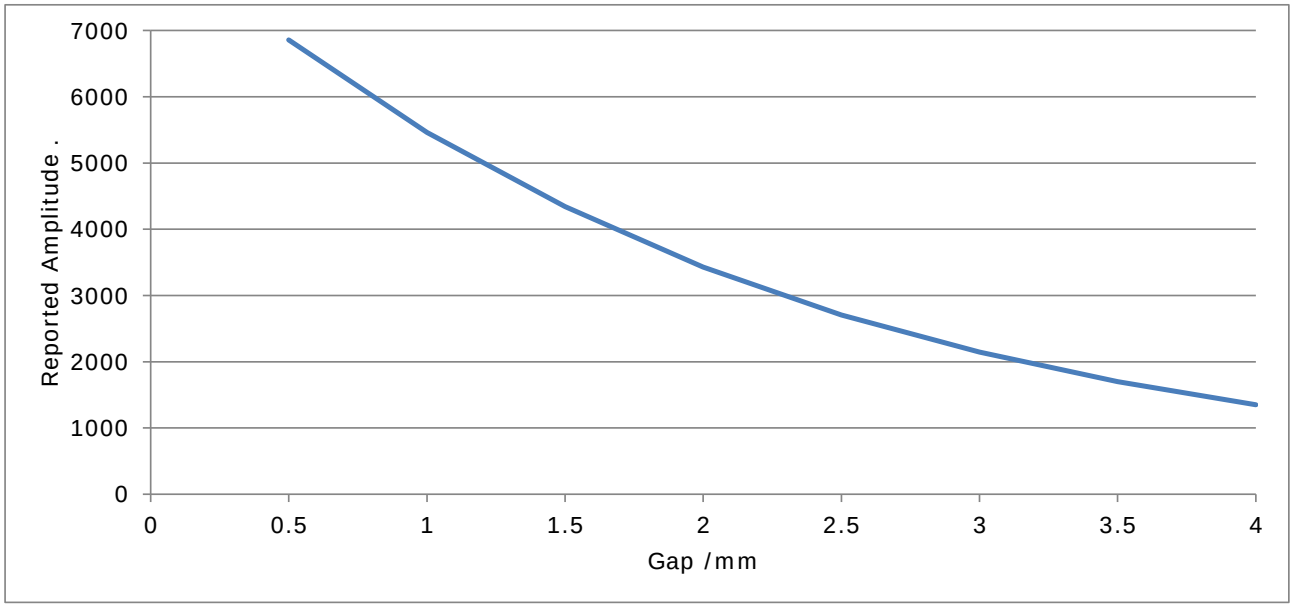


Figure 19 Minimum Reported Amplitude as a function of Gap, free space

5.3 Noise Free Resolution

Noise Free Resolution is defined in section 4.4. It is a function of the signal level detected by the CTU chip. It therefore reduces with gap in a similar way to Reported Amplitude as illustrated in Figure 20.

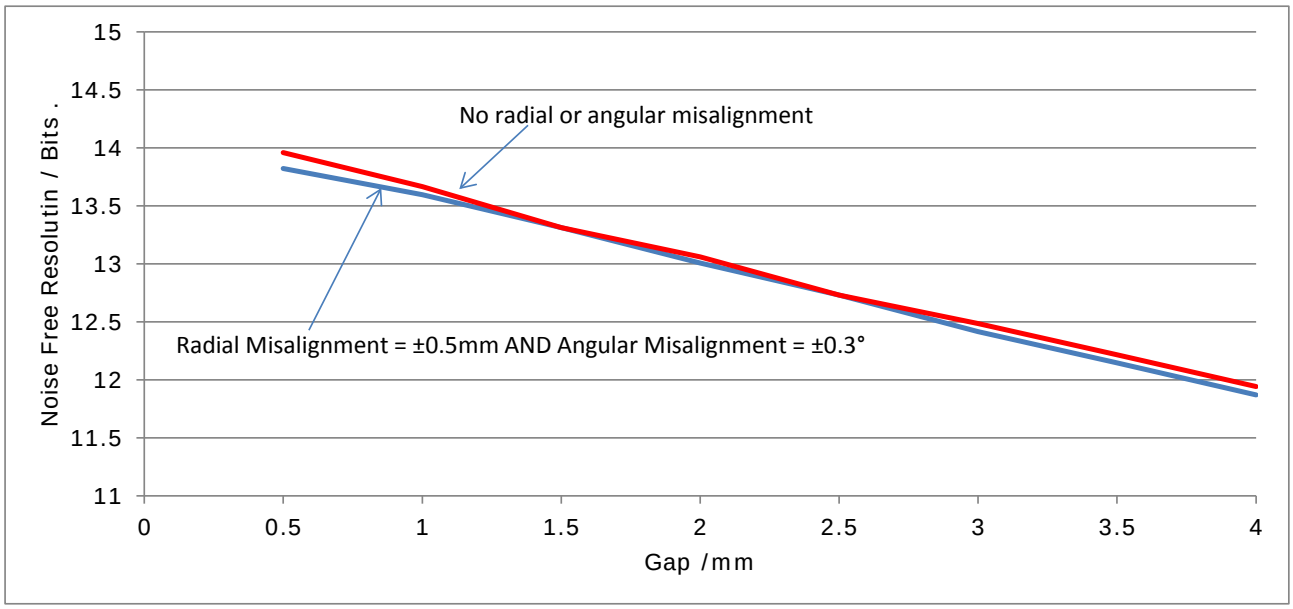


Figure 20 Noise Free Resolution as a function of Gap, CAM204 CTU chip, free space

Quoted Noise Free Resolution is based on single measurements from a CTU chip. The host may average (or otherwise digitally filter) measurements to yield a higher resolution than shown above, at the expense of greater latency.

© Cambridge Integrated Circuits Ltd 2012-2016

5.4 Immunity to Misalignment

Section 4.6 defines how immunity to radial misalignment between target and sensor axes can be quantified, and results for the 35mm Type 6.3 Rotary Sensor are presented in Table 4.

Table 4 Immunity to Misalignment

Parameter	Value
Measured Sensitivity to Radial Misalignment, worst case across Actual Angle, misalignment direction, Gap up to 4mm and Angular Misalignment up to 0.3°	0.16°/mm
Radial Misalignment Rejection Ratio	29

5.5 Maximum Misalignment

When used with the target design detailed in section 3 the sensor will report angle correctly even when the target and sensor are badly misaligned. Table 5 shows the maximum allowable misalignments, and the resulting maximum linearity error. If radial or angular misalignment exceeds these values, for example when held by hand during demonstration, reported position may include an error of ±120° if valid.

Table 5 Maximum misalignment between target and sensor

Parameter	Maximum
Radial Misalignment	1.4mm
Angular Misalignment	1.4°
Gap	3.5mm (CAM204 CTU chip) 3mm (CAM502 CTU chip)
Linearity Error at max misalignments	0.6°

© Cambridge Integrated Circuits Ltd 2012-2016

6 Metal Integration

6.1 Background

As with all resonant inductive sensors, the 35mm Type 6.3 sensor and its target can be integrated near metal providing the metal's influence is not excessive.

Nearby metal can cause additional linearity error, although the effect is usually small, especially when the metal is placed symmetrically around the sensor.

The metal must not dampen the resonator's Q-factor excessively, and distort fields such that coupling factor is reduced excessively, otherwise Amplitude will be significantly reduced. Low Amplitude causes low Noise Free Resolution. When Amplitude is reduced to 50% of its original value, Noise Free Resolution will reduce by approximately 1 bit. In extreme cases Amplitude may fall below the CTU chip's minimum Amplitude for reporting VALID.

The target's resonant frequency Fres when integrated with the customer's product must also remain within the tuning limits of the CTU it will be used with, typically 187.5kHz ±7% for the CAM204. Fres is a function of the metal environment inside the product. When there is very little metal nearby, Fres will equal the target's free space resonant frequency. When there is metal nearby, Fres will shift. For non-ferrous, highly conductive materials such as aluminium and brass, Fres increases as metal approaches. If the shift is substantial, it may be necessary to alter the nominal free space resonant frequency so that when integrated with the product Fres remains within the CTU's tuning range. The free space resonant frequency may be lowered by increasing the target's resonating capacitance CRES of Figure 13.

Small metal objects such as fixing screws have less effect than larger objects and metal surfaces. The sensor 013-0024 can be mounted using steel M2 screws with barely noticeable effect on Amplitude, for example.

The effect of a product's fixed metal environment is highly reproducible and can be established by experiment, for example using CambridgeIC's CTU Demo application and appropriate sensor, target and CTU Development Board.

Large areas of aluminium, brass or copper near the sensor and target can be tolerated, as illustrated in the following subsections. However these materials must be at least 0.2mm thick, otherwise their conductivity is insufficient to repel magnetic fields efficiently and Amplitude is reduced more than the values illustrated.

The sensor and its target tolerate aluminium and brass nearby much better than steel, iron, titanium or stainless steel. It is recommended to cover any large areas of iron, titanium or stainless steel near the sensor and target with an aluminium screen at least 0.2mm thick. For example if there is a steel shaft passing through the middle of the sensor and target, it should preferably be shrouded in an aluminium tube with wall thickness 0.2mm or more.

Please refer to the CambridgeIC white paper "Resonant Frequency Centering" for more details, including practical approaches for testing and analysis.

The following sections illustrate the effect of aluminium parts near the sensor and target. Brass and copper will behave similarly.

© Cambridge Integrated Circuits Ltd 2012-2016

6.2 Between Aluminium Plates, Target Mounted to Aluminium

In the example illustrated in Figure 21 the 35mm Type 6.3 Rotary Sensor and transponder coil target PN 013-1019 operate between parallel aluminium plates. The target is mounted direct to aluminium, and there is a variable gap between sensor and aluminium behind.

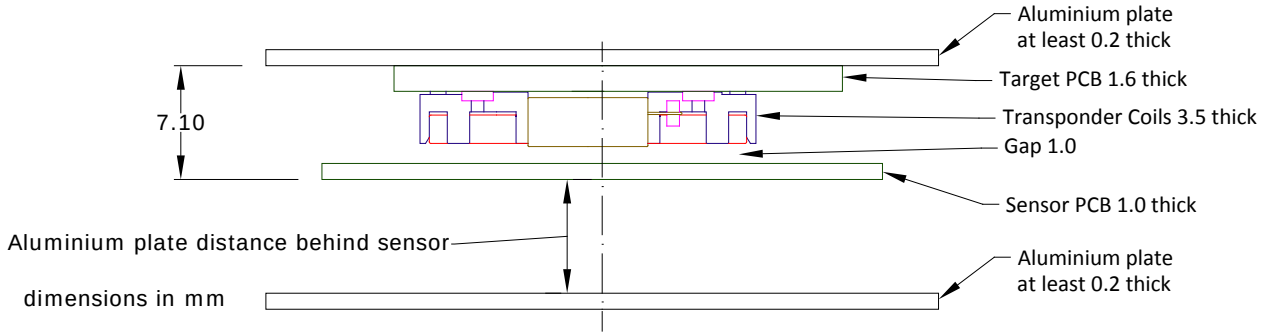


Figure 21 Between Aluminium Plates, Target Mounted to Aluminium

Figure 22 shows how reported Amplitude and frequency change with the aluminium plate distance behind the sensor. The left hand axis is for the Amplitude shown in blue, and the right hand axis is for frequency in red.

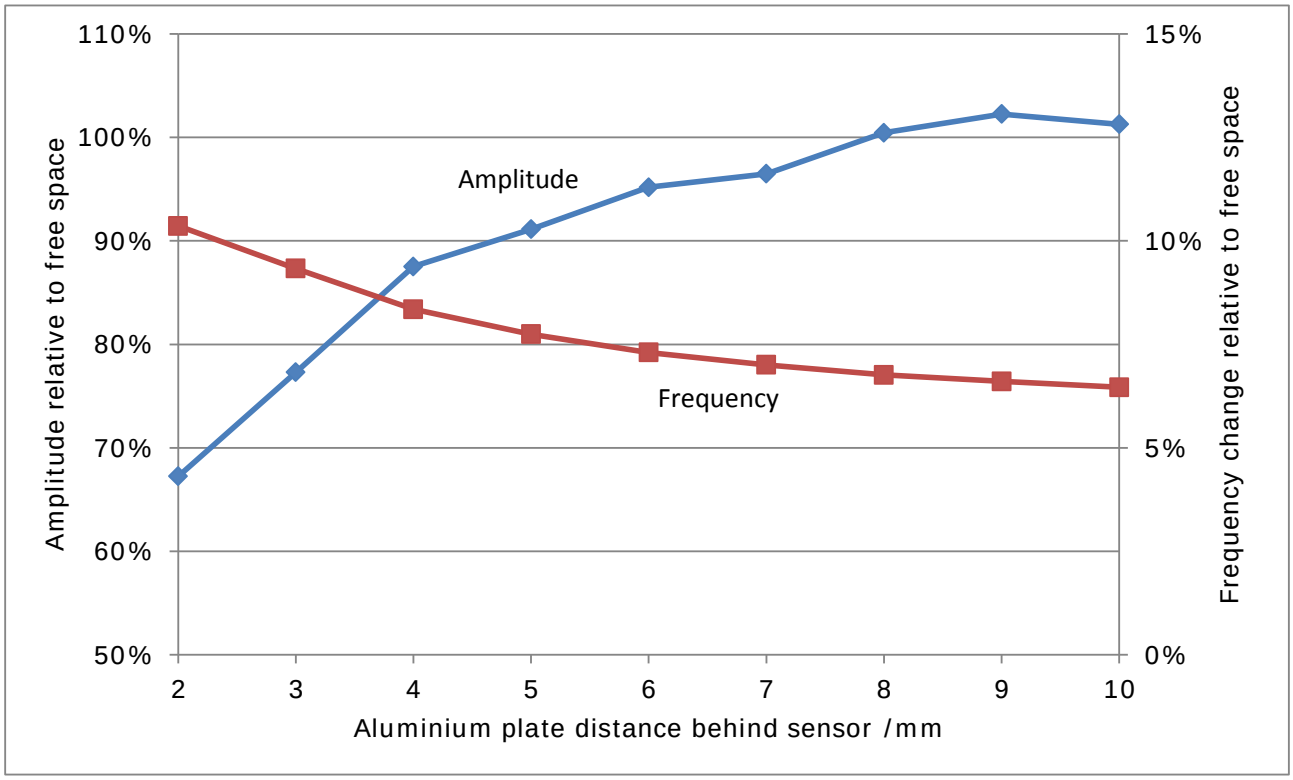


Figure 22 Effect of nearby aluminium on Amplitude and Resonant Frequency

© Cambridge Integrated Circuits Ltd 2012-2016

6.3 Between Aluminium Plates, Target Mounted to Aluminium, With Rod

The example of Figure 23 is similar to that of the previous section, except there is also an aluminium rod passing through both sensor and target.

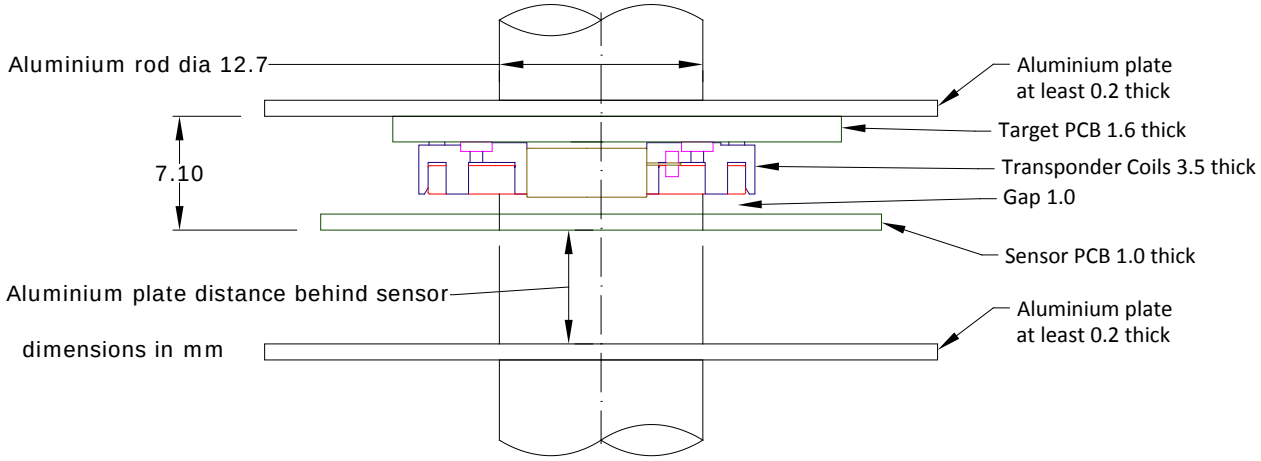


Figure 23 Between Aluminium Plates, Target Mounted to Aluminium, With Rod through Centre

Figure 24 shows how reported Amplitude and frequency change with the aluminium plate distance behind the sensor. There is a greater reduction in Amplitude and a greater increase in frequency than shown in Figure 22, due to the presence of the aluminium rod in addition to the two plates.

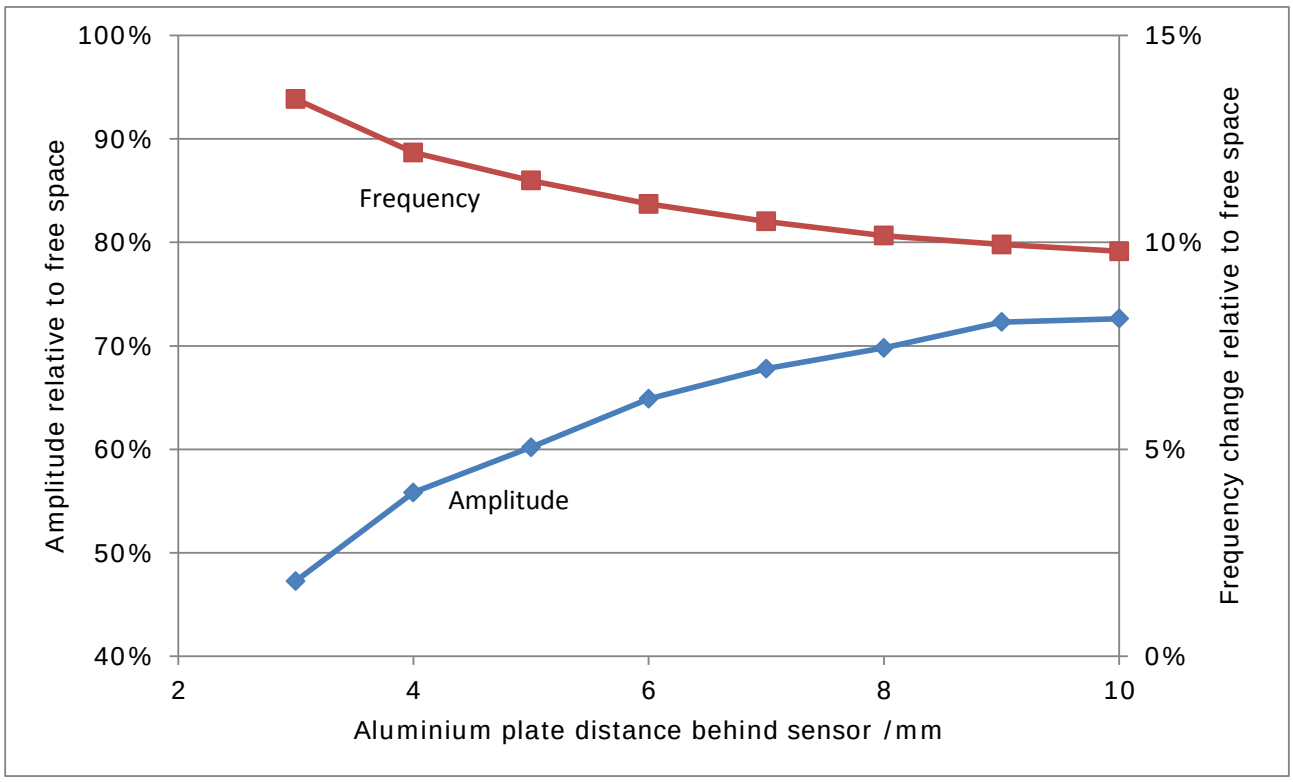


Figure 24 Effect of nearby aluminium on Amplitude and Resonant Frequency

© Cambridge Integrated Circuits Ltd 2012-2016

6.4 Between Aluminium Plates, Sensor 2mm Above Aluminium

The example of Figure 25 is similar to Figure 21, except the sensor is positioned a fixed 2mm from the nearest aluminium plate and the distance between target and aluminium is varied instead.

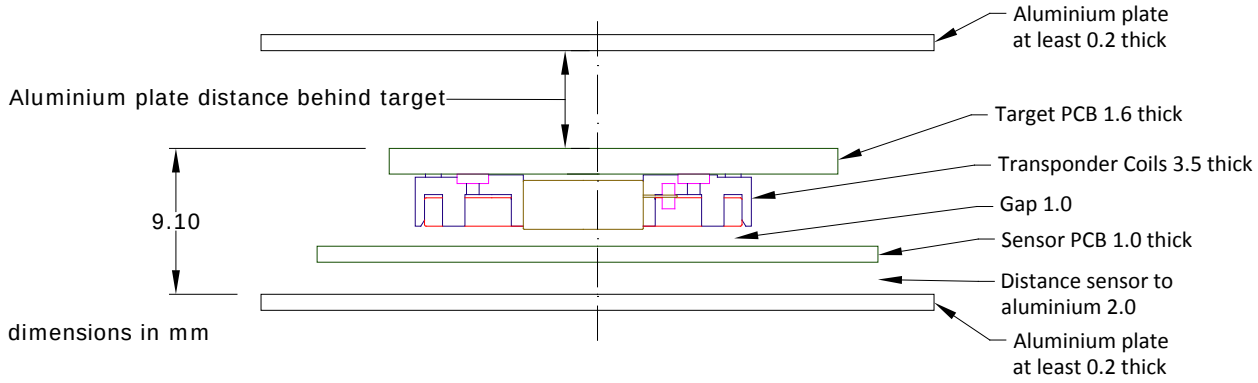


Figure 25 Between Aluminium Plates, Sensor 2mm Above Aluminium

Figure 26 shows how reported Amplitude and frequency change with the aluminium plate distance behind the target.

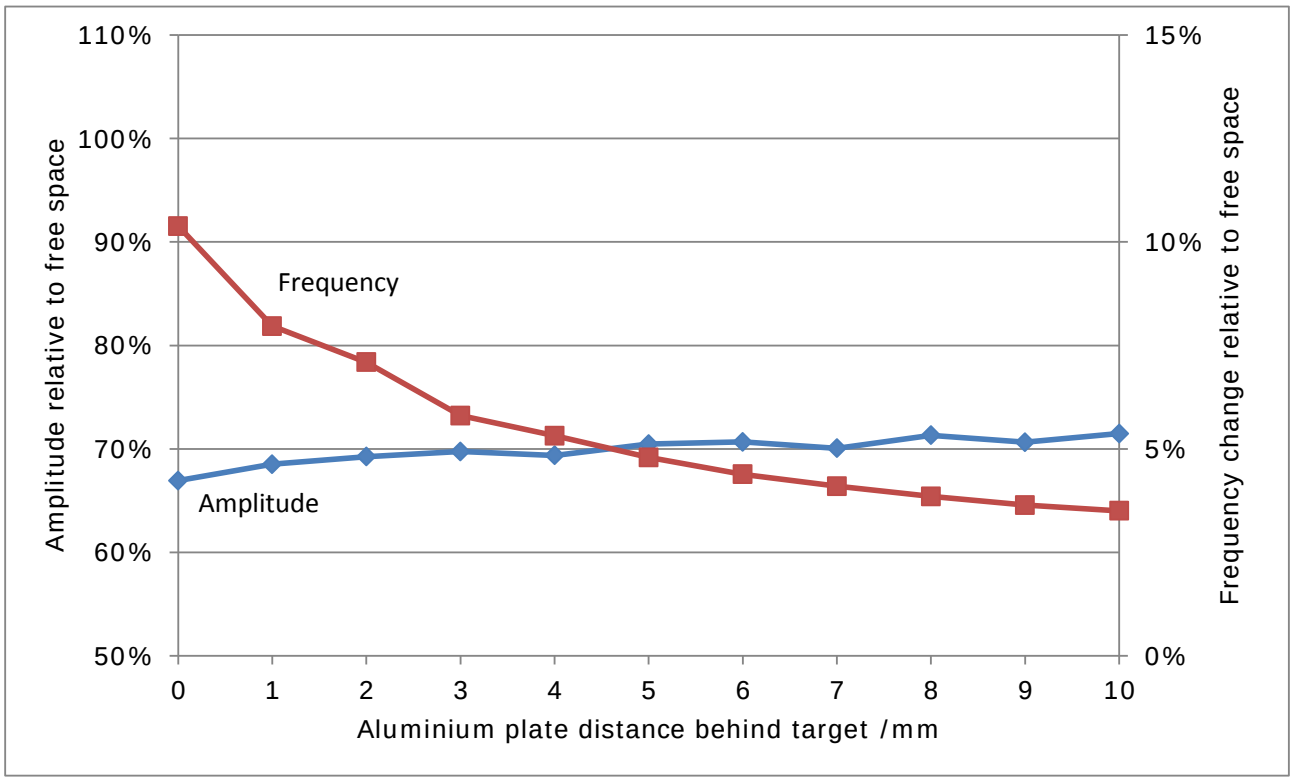


Figure 26 Effect of nearby aluminium on Amplitude and Resonant Frequency

© Cambridge Integrated Circuits Ltd 2012-2016

6.5 Between Aluminium Plates, Sensor 2mm Above Aluminium, With Rod

The example of Figure 27 is similar to Figure 25, except there is also an aluminium rod passing through both sensor and target.

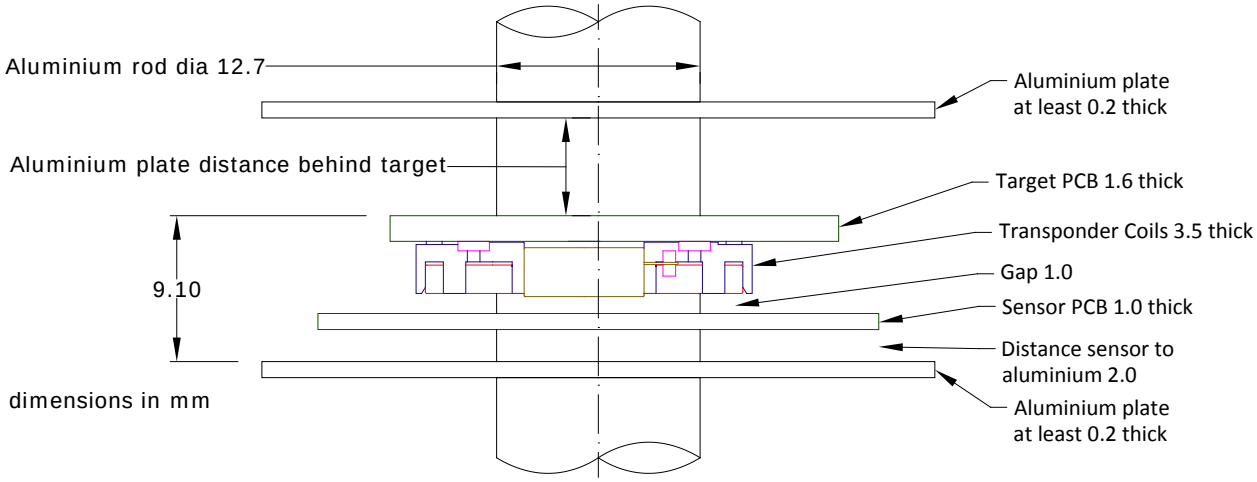


Figure 27 Between Aluminium Plates, Sensor 2mm Above Aluminium, With Rod Through Centre

Figure 28 shows how reported Amplitude and frequency change with the aluminium plate distance behind the target in this case. There is a greater reduction in Amplitude and a greater increase in frequency than shown in Figure 26, due to the presence of the aluminium rod in addition to the two plates.

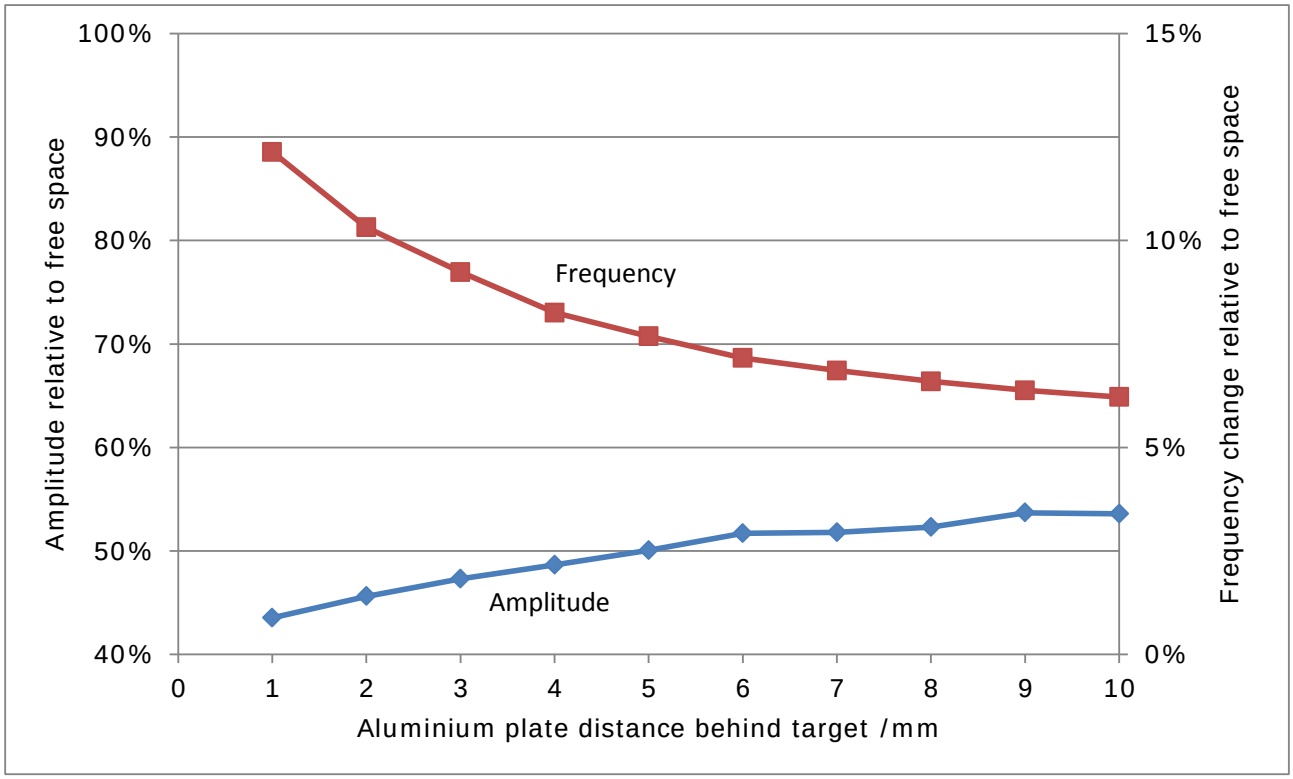


Figure 28 Effect of nearby aluminium on Amplitude and Resonant Frequency

© Cambridge Integrated Circuits Ltd 2012-2016

7 Operation at Temperature Extremes

7.1 Position Stability across Temperature

Reported position from the 35mm Type 6.3 Sensor is extremely stable with temperature, because angle measurements are closely related to the physical geometry of the coils and these are stable due to the PCB process. CTU processing chips like the CAM204 and CAM502 introduce very little additional error because their operating principle is fully ratiometric and they are tolerant of Amplitude and frequency changes.

Figure 29 is a plot of change in reported position from its initial value at 20°C, for a typical 35mm Type 6.3 Sensor used with target PN 013-1019 at 1mm Gap and a CAM204 processing chip. The relative position of sensor and target are fixed. All parts including the CAM204 were at approximately the same temperature, although this is not a requirement for temperature stability because they operate independently. Measurements were taken at several angles, and the one presented here has the worst deviation across 360°.

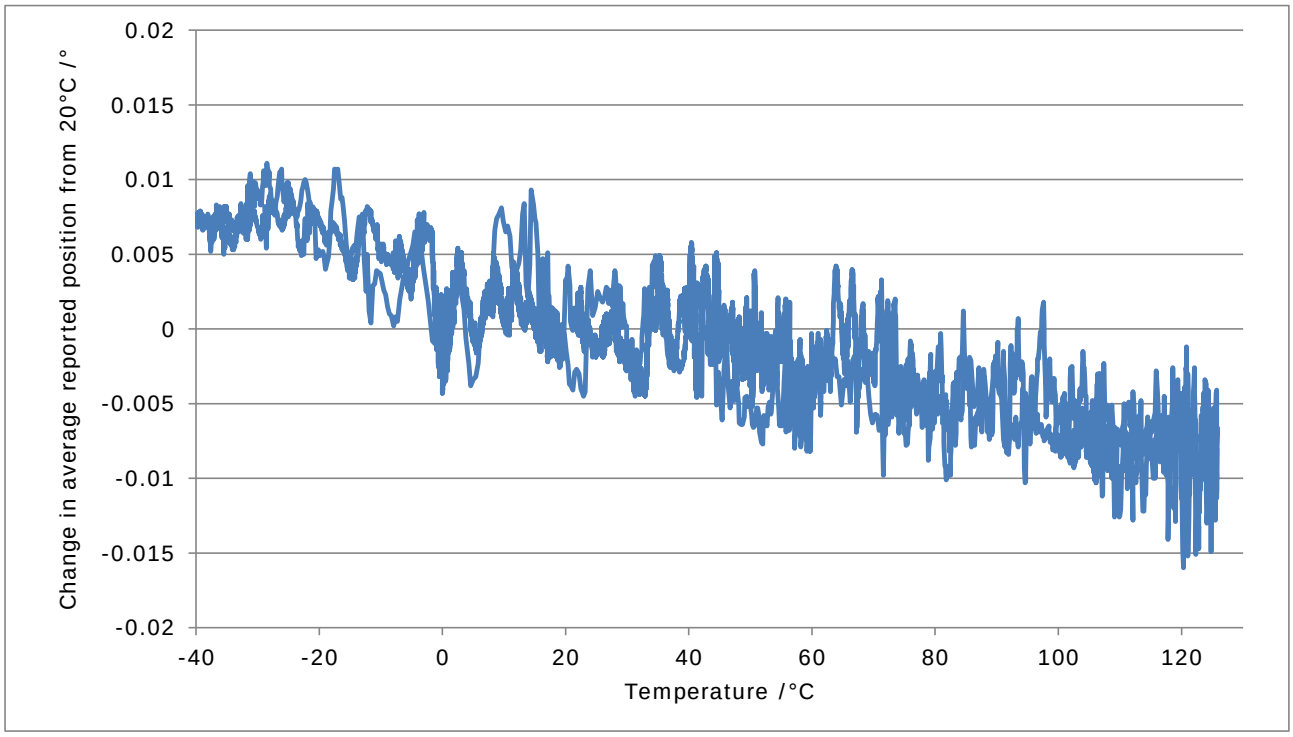


Figure 29 Temperature stability of reported position, processing with CAM204 chip, 1mm Gap

Measurements started at 20°C, then temperature was reduced -40°C, then increased to +125°C and finally reduced back to 20°C again. Note that there is no thermal hysteresis: the final measurements at 20°C coincided with the first ones.

There is a very small slope to the temperature dependence, on the order of 0.0012°/°C. Most likely this is due to a difference in the rate of thermal expansion in the FR4 substrate in orthogonal directions, because FR4 material is not perfectly anisotropic.

The temperature dependence is slightly “noise-like”, with deviations of ±0.005° (“15 bit level”) for temperature changes of a few degrees. This is due to resonator frequency change and the CAM204 frequency tuning process.

For the above measurements the target was fixed relative to the sensor. In practical systems the two are mounted on separate parts which may also move axially and radially relative to one another, and those movements may also be temperature dependent. As an example, a rotating shaft’s axis may shift radially by 10µm across temperature. The maximum effect of this position change on the 35mm Type 6.3 rotary sensor is then 10µm x 0.16°/mm (Table 4) = 0.002°. On the other hand, an optical encoder or off-axis magnetic encoder of similar size will experience a change about 29 times greater (Radial Misalignment Rejection Ratio, Table 4). That is, by 0.05°.

© Cambridge Integrated Circuits Ltd 2012-2016

7.2 Effect of Temperature on Amplitude and Noise Free Resolution

Reported Amplitude changes with temperature, as illustrated in Figure 30. Most of the reduction at high temperature is due to the lower Q-factor of the resonator in the target, which is in turn due to higher coil resistance.

Noise Free Resolution reduces with Amplitude. For example Amplitude reduces to 65% of its 20°C value at +125°C, and this in turn reduces Noise Free Resolution by 0.6 bits.

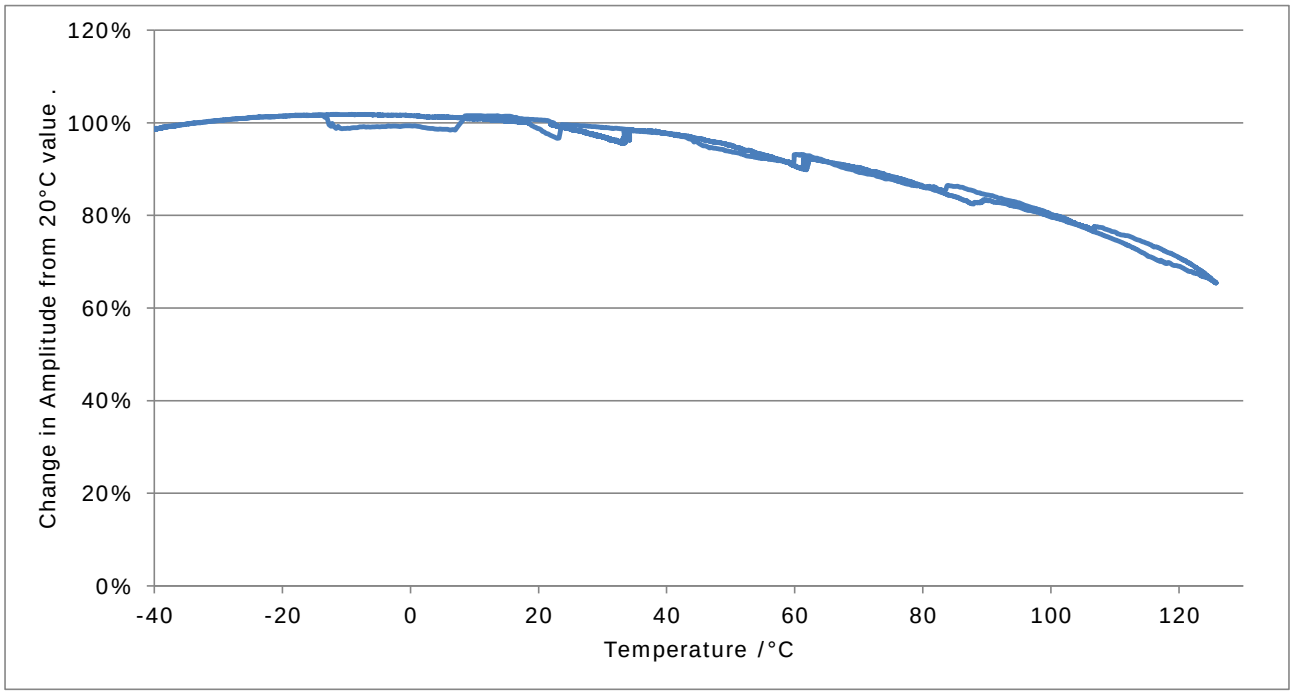


Figure 30 Amplitude change with temperature, processing with CAM204 chip, 1mm Gap

7.3 Effect of Temperature on Target Frequency

The resonant frequency of the target will change with temperature. The maximum change for assembled targets PN 013-1019 is specified in Table 3. CTU chips tolerate a relatively wide resonator frequency range. However care should still be taken to ensure the frequency of targets remains inside the tuning range of the CTU chip, while also considering the effect of metal (section 6). Please see the white paper “Resonant Frequency Centering” for more details.

© Cambridge Integrated Circuits Ltd 2012-2016

8 Operation at High Rotation Speed

8.1 Mechanical

Table 6 includes maximum speeds for mechanical integrity. It is strongly recommended to avoid use at higher speeds.

Table 6 Maximum rotation speed, mechanical

Condition	Max Speed	Failure mode above quoted max
Mechanical limit, target 013-1019, -40°C…+125°C	10,000 rpm	Transponder coil mounts distort Parts may fly off PCB

WARNING: Targets built by CambridgeIC may not be used where their mechanical failure might reasonably be expected to result in personal injury. An appropriate guard must always be used to protect against mechanical failure, any time parts are rotated at sufficient speed to cause injury. These apply even when parts are operated below any maximum speeds quoted in Table 6.

8.2 Functional, CAM204 CTU Chip

CambridgeIC's CAM204 CTU chip is usually for slow speed applications due to its relatively large Group Delay (500us when INCF=1). For rotation speeds above a few hundred rpm the CAM502 is recommended. However the CAM204 will operate the 35mm Type 6.3 Sensor at moderate speeds as shown in Table 7.

Table 7 Maximum rotation speed, CAM204

Condition	Max Speed	Failure mode above quoted max
Rotation while CAM204 resets then starts sampling, Sample Interval 2000us, INCE=1	3,000 rpm	Persistent fine skipping error
Rotation once already sampling and VALID, INCE=1, Sample Interval 1000us, INCE=1	6,000 rpm	Persistent fine skipping error
INCE=0	4,800 rpm	Amplitude reduces by more than 20% from static value

8.3 Functional, CAM502 CTU Chip

CambridgeIC's CAM502 CTU chip is capable of high speed operation. Please refer to its datasheet for full details. When used with the 35mm Type 6.3 Sensor the maximum operation speeds are as shown in Table 8. The maximum speed depends on how the CAM502 chip is used and configured, and a selection of typical use cases is illustrated below. Note that they all use a minimum measurement interval of 200us, which delivers greatest allowable speeds.

Table 8 Maximum rotation speed, CAM502

Condition	Max Speed	Failure mode above quoted max
Rotation while CAM502 resets then starts sampling, Pipeline Interval 200us, INCE=1	6,000 rpm	Persistent fine skipping error
Rotation once already sampling, Pipeline Interval 200us, INCE=1	40,000 rpm	Persistent fine skipping error
Pipeline Interval 200us, INCE=0	20,000 rpm	Fine skipping error
Continuous Pipeline Measurement, Sample Interval 200us, INCE=0	20,000 rpm	Fine skipping error

Note that maximum speeds quoted in Table 8 are in excess of the mechanical capabilities of targets, see section 8.1 and its warnings.

© Cambridge Integrated Circuits Ltd 2012-2016

9 Sensor Blueprint 010-0057

9.1 Purpose

A Sensor Blueprint is data defining the pattern of conductors for building the sensor onto a PCB. A customer may build their own sensors for use with CambridgeIC's CTU chips, either as stand-alone sensors or combined with their own circuitry.

9.2 Fabrication Technology

The Sensor Blueprint is fabricated on a 6-layer PCB. Recommended copper thickness is shown in Table 9.

Table 9

Copper thickness	**oz**	**µm**
Minimum	0.8	28
Recommended	1	35

9.3 PCB Design Parameters

Table 10

PCB Design Rules	**Minimum values used**	
	mm	inches
Track width	0.2	0.0079
Gap between tracks	0.2	0.0079
Via land outer diameter	0.8	0.031
Drill hole diameter	0.4	0.016

9.4 PCB Integration

Figure 31 illustrates the extent of the copper pattern required to build the sensor on a PCB. The shaded area is the sensor itself, with coil connections shown to the upper right. The coil pattern may be rotated or flipped to fit a customer's assembly, in which case the position reported by the CTU will be transformed accordingly.

When integrating with other electronic circuitry, a keep-out of 3mm is recommended all round the sensor's conductors.

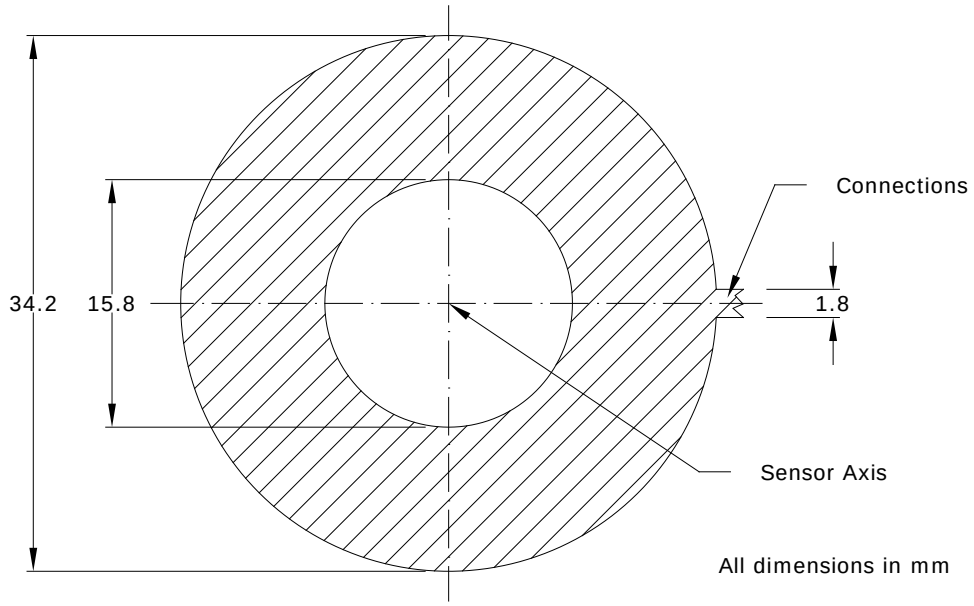


Figure 31 Copper extent

© Cambridge Integrated Circuits Ltd 2012-2016

9.5 Data Format

The Sensor Blueprint is supplied as Gerber data in RS-274-X format with the following settings: imperial, 2.4 precision and leading zero suppression. Coordinates are relative to the Sensor Axis.

9.6 Trace Connections

There are 5 pairs of tracks (EX, COSA, SINA, COSB, SINB and their respective VREF connections), which should be connected to the respective CTU circuit connections with the minimum practical trace lengths.

Please refer to the CAM204 datasheet for recommendations on track design for connecting sensors to CTU circuitry.

© Cambridge Integrated Circuits Ltd 2012-2016

10 Environmental

Assembled sensor part number 013-0024 conforms to the following environmental specifications:

Item	Value	Comments
Minimum operating temperature	-40°C	Limited by the wire used for connections
Maximum operating temperature	85°C	
Maximum operating humidity	85%	Non-condensing

The maximum operating temperature may be increased if a customer manufactures their own sensor PCB to CambridgeIC's design, and uses an alternative, higher temperature, connecting method.

11 RoHS Compliance

CambridgeIC certifies, to the best of its knowledge and understanding that part numbers 013-0024 and 013-1019 are in compliance with EU RoHS, China RoHS and Korea RoHS.

12 Document History

Revision	Date	Comments
0001	2 March 2016	First draft based on 033-0033, for 35mm Type 6.3 sensor using discrete ferrite rods.
0002	1 April 2016	Added operation at high speed and temperature extremes.

13 Contact Information

Cambridge Integrated Circuits Ltd
21 Sedley Taylor Road
Cambridge
CB2 8PW
UK

Tel: +44 (0) 1223 413500

info@cambridgeic.com

14 Legal

This document is © 2012-2016 Cambridge Integrated Circuits Ltd (CambridgeIC). It may not be reproduced, in whole or part, either in written or electronic form, without the consent of CambridgeIC. This document is subject to change without notice. It, and the products described in it ("Products"), are supplied on an as-is basis, and no warranty as to their suitability for any particular purpose is either made or implied. CambridgeIC will not accept any claim for damages as a result of the failure of the Products. The Products are not intended for use in medical applications, or other applications where their failure might reasonably be expected to result in personal injury. The publication of this document does not imply any license to use patents or other intellectual property rights.

The design of the sensor, comprising each of the patterned copper layers, drill locations, silk screens, assembly layers and board outline are protected by copyright.

The parts described in this datasheet are subject to the following patents: US8570028, GB2461448, GB2488389 and GB2500522. Other patents are pending.